International Journal of Heat and Fluid Flow 30 (2009) 789–795

Contents lists available at ScienceDirect

International Journal of Heat and Fluid Flow

journal homepage: www.elsevier.com/locate/ijhff

On the quantification of preferential accumulation

Stephen J. Scott [a], Aditya U. Karnik [b], John S. Shrimpton [b,*]

[a] Multi-Scale Fluid Dynamics Group, Dept. Mechanical Engineering, Imperial College London, South Kensington, London SW7 2AZ, United Kingdom
[b] Energy Technology Research Group, School of Engineering Sciences, University of Southampton, Southampton, S017 1BJ, United Kingdom

ARTICLE INFO

Article history:
Received 9 April 2008
Received in revised form 5 February 2009
Accepted 6 February 2009
Available online 13 March 2009

Keywords:
Isotropic
Turbulence
Particle
Preferential accumulation

ABSTRACT

It is well-known that heavy particles in homogeneous isotropic turbulence tend to collect in certain regions of the flow, leading to preferential accumulation. In this study, we investigate different measures of preferential accumulation, some of which show a dependence on Reynolds number. All the measures used in this study confirm that this phenomenon is most pronounced for a Stokes number, $St \sim 1$, based on the Kolmogorov time-scale. The variation with Stokes number has been studied over a wider range for all the measures than in previous studies. Though the effect of changing St, for a particular Re, has been well understood, the scaling with Re is not so obvious. The measures used in this study seem to suggest a structure to the particle concentration field which scales with Re. To investigate this structure, we introduce a concentration distribution length scale which shows a dependence on Re, especially at higher St. The results in the present work agree with several previous computational and experimental works and provide a more unified picture of the dependence of preferential accumulation on St and Re.

1. Introduction

Direct numerical simulations of dispersed phase flows, using the point-particle assumption for particles, have proved very useful to probe the particle distribution characteristics. Depending on whether the effect of particle phase on the fluid phase has been neglected or incorporated, the simulations are classified as one-way coupled and two-way coupled respectively. Direct numerical simulations have been widely used to investigate both one-way (Elghobashi and Truesdell, 1992) and two-way coupled (Boivin et al., 1998) situations in homogeneous turbulence. In this study, we focus our attention on one-way coupled situations. The DNS code using point-particles, described within this paper, simulates the simplest case of stationary homogeneous isotropic turbulence (HIT) and one-way coupling and is used to investigate small-scale turbulence effects on preferential accumulation. Complete details of the code mathematical background may be obtained from Scott (2006).

It has been shown in a series of papers, both numerical and experimental, that inertial particles tend to accumulate in areas of high-strain and low vorticity. This phenomenon is generally referred to as preferential accumulation or preferential concentration (henceforth referred to as PC) in literature. The clustering of particles or droplets plays an inherently important role in processes like droplet formation in clouds (cf. review by Shaw (2003)) and coagulation of particles caused by collisions (Wang et al. 2000). In this study, we use different measures for quantifying preferential concentration and probe their dependence on Stokes number (St) and Taylor Reynolds number (Re).

Before proceeding to discuss observations on PC in literature, we define here the various measures of accumulation encountered in this study for the benefit of the reader. Some of the measures, introduced elsewhere in literature are re-defined here for purpose of clarity and some new measures are introduced here. The D_c measure, introduced by Wang and Maxey (1993), is a bin-size dependent measure defined as follows:

$$D_c = \sum_{C=0}^{N_p} \left(P_c(C) - P_c^u(C)\right)^2 \tag{1.1}$$

where the concentration C is the number of particles found in a small cube with its side equal to the specified bin-size and N_p is the total number of particles. $P_c(C)$ is the measured probability of finding a small cube with concentration C and $P_c^u(C) = e^{-\lambda}\lambda^C/C!$ is the same for a Poisson distribution (Squires and Eaton, 1990a) with mean particle number density λ. Another measure of quantifying the deviation from random distribution is the D measure (Fessler et al., 1994) defined as follows:

$$D = \frac{\sigma - \sigma_{Poisson}}{\lambda} \tag{1.2}$$

where σ and $\sigma_{Poisson}$ represent the standard deviations for the measured particle number density distribution and the Poisson distribution. Both the D and D_c measures characterize the deviation of the observed particle distribution from a perfectly random distribution. For a random distribution of particles, both D and D_c would be equal to zero. The correlation dimension, D_2, introduced by Grassberger

* Corresponding author.
E-mail address: john.shrimpton@soton.ac.uk (J.S. Shrimpton).

0142-727X/$ - see front matter © 2009 Elsevier Inc. All rights reserved.
doi:10.1016/j.ijheatfluidflow.2009.02.002

and Procaccia (1983), is part of a spectrum of generalized dimensions used to characterize multifractal sets. The correlation dimension is defined as follows:

$$D_2 = \lim_{l \to 0} (1/\log l) \log \sum p_i^2 \tag{1.3}$$

where l is a variable length scale and p_i is the probability that the separation distance between two particles is less than l (Tang et al., 1992). We compute this quantity by binning all of the particle pairs $N(l)$, according to their separation distance l, and calculating the slope of the curve $\log(N(l))$ versus $\log(l)$ over a range of l where a linear dependence exists. For a uniform distribution of particles, D_2 equals the space dimension (three in our case). In the present study, we introduce a measure which correlates the local particle number density concentration to the local fluid enstrophy (referred henceforth as ND-E correlation). The ND-E correlation is defined as $\langle n'e' \rangle / \langle n \rangle \langle e \rangle$ where $\langle n \rangle$ and $\langle e \rangle$ are the mean particle density and the mean enstrophy respectively. All the averages $\langle\,\rangle$ in the preceding definition refer to Eulerian averages over the simulation domain. It follows from the definition that preferential concentration of particles in low-enstrophy areas would result in increasingly negative values of the ND-E correlation. Another measure introduced in the present study is the clustering length scale, l_n, defined as follows:

$$l_n = \frac{\pi}{2\langle n \rangle^2} \int \frac{\hat{N}(\kappa)}{\kappa} d\kappa \tag{1.4}$$

where $\hat{N}(\kappa) = 1/2\langle \hat{n}(\kappa)\hat{n}^*(\kappa) \rangle$ is defined on lines of fluid kinetic energy to obtain a length scale consistent with fluid integral length scale. This length scale provides a convenient measure of the extent of the region over which the number density field is correlated.

Typically radial distribution function (RDF), introduced by Sundaram and Collins (1997) and correlation dimension (D_2) have been used to quantify the multi-scale nature of the particle distribution. The measures can be broadly divided into two types – the D and D_c measures quantify the deviation of the particle distribution from randomness, while the correlation dimension, D_2 is a measure of particle–particle separation. In this study, we take a closer look at what each of these measures represent. While the global measures like D, D_c quantify the global property of distribution, multi-scale measures like RDF and D_2 probe the structure of particle distribution from a fractal point of view. As such, D and D_c measures tend to depict uniform particle distribution at higher Reynolds numbers while D_2 exhibits independence with Reynolds number. Also, in this study, we cover a wider range of Stokes numbers for all the measures of accumulation than in any previous study. In addition to the measures mentioned above, we introduce a couple of new measures – ND-E correlation and the clustering length scale, l_n, to better understand the structure of PC.

Squires and Eaton (1991) demonstrated PC in isotropic turbulence ($Re = 38.7$) and found that particles are most preferentially accumulated for the intermediate Stokes number in their simulations. Wang and Maxey (1993) investigated concentration distribution of particles at $Re = 31$. They introduced the D_c measure for quantifying local accumulation and found PC to be a Kolmogorov scale phenomenon. In their experimental investigation, Fessler et al. (1994) calculated the D parameter for quantifying PC and investigated the role of box-size used for calculating the D parameter. They noted that evaluating the dependence of D on box-size revealed useful information about the scale on which PC occurs. Eaton and Fessler (1994) summarized the mechanism of PC in their review, attributing it primarily to the coherent vortical structures present in the fluid. At the lower Reynolds numbers used in the studies mentioned before, PC is mainly influenced by the action of Kolmogorov scale eddies. This phenomenon has been captured in numerous studies using measures of deviation from randomness like D and D_c. It is well-known and consistently observed that PC is most pronounced for Stokes number, $St \sim 1$, where St is based on the Kolmogorov time scale.

Many recent studies have pointed to the multi-scale nature of preferential concentration phenomenon at higher Reynolds numbers. Goto and Vassilicos (2008) have pointed out the role of multi-scale eddies in PC at higher Reynolds numbers. The 'sweep-stick' mechanism proposed by them, points to the tendency of particle clusters to reflect the underlying acceleration structure of the fluid flow field. Chen et al. (2006) found a good correlation between acceleration stagnation points of fluid and particle clusters for particle response times smaller than integral scale of turbulence in 2D turbulence. This upper limit on particle response time corresponds to $St \sim 15$ for the highest Re in the present simulations. Yoshimoto and Goto (2007) demonstrated the role played by eddies of the size range between Kolmogorov and integral length scales of the flow on clustering.

Van Aartrijk and Clercx (2008) used the correlation dimension (D_2) as a measure of accumulation and investigated PC in both HIT and stratified turbulence. They concluded that PC is only weakly dependent on Re. Similar conclusion was reached by Collins and Keswani (2004) and Hogan and Cuzzi (2001). Collins and Keswani (2004) studied the scaling of radial distribution function (RDF), first introduced by Sundaram and Collins (1997) in the context of particle collisions, with Reynolds number. They found that the RDF saturates to a constant value with increasing Re, for the range of Re (65–152) in their study. Bec et al. (2007) probed the dependence of PC on Reynolds number using DNS. They point out that PC is independent of Re at the dissipative scales, but the same argument does not apply at higher Re, where a much broader range of length and time scales are involved. In particular they note the direct relationship between particle distribution and structure of acceleration field in the inertial range. Balkovsky et al. (2001) also point out the scale invariance at small scales, but note that deviations from uniform distribution for higher St, are expected to depend on the scales involved. The scale invariance of clustering at dissipative scales is also observed in 2D turbulence by Boffetta et al. (2004). They suggest that clustering of particles relates to the presence of structures characterized by a large set of time scales.

In their experiments, Aliseda et al. (2002) characterize PC using D and D_c measures introduced earlier and also probe the role of bin-size on these measures. In their study, a bin-size on 10η corresponds to the peak of these measures, consistent with similar earlier observation by Fessler et al. (1994) in their experiment (note: $Re \sim 75$ in Aliseda et al., $Re \sim 150$ in Fessler et al.). Though the study by Aliseda et al. gives a detailed account of clustering characteristics for a particular Re, being limited to a single Re, the scaling with Re remains unexplored in their study. Wood et al. (2005) conduct experiments at much higher Re ($Re \sim 230$), where PC occurs over a fairly wide range of scales. The bin-size dependence of D measure suggests a peak around bin-size of $8–20\eta$, which is a broader range than found in experiments by Aliseda et al. and Fessler et al. at lower Re. Wood et al. also observed that this peak shifts towards larger length scales for higher Stokes numbers.

It has been established that multi-scale eddies play an increasingly important role in preferential accumulation at higher Reynolds numbers. In this study, we introduce a clustering length scale for particle concentration, similar to integral scale for the fluid. Such a measure would give an estimate of the spacing between particle clusters. Combined with studying the bin-size dependence of D and D_c measures for different Reynolds number, it enables us to gain a better understanding of scaling of the clustering phenomenon with Re. Also we look at the D_2 measure, to facilitate comparison with studies focusing on scaling of RDF with Reynolds number.

The remainder of this manuscript is organized as follows. Section 2 presents abridged details of the pseudo-spectral method, code organization, initialization, forcing method and validation. In Section 3, results from a comprehensive set of mono-sized simulations are presented. Section 4 discusses these results in the context of recent computational and experimental work, which used different measures of preferential accumulation to add some further illumination to our arguments. Finally, the main findings are summarized in the concluding remarks.

2. Continuum phase method

The pseudo-spectral method (Orszag and Patterson, 1972), as described by Rogallo (1981) has been used to simulate the fluid turbulence. In the pseudo-spectral method, the non-linear term is evaluated in real space and transformed back to Fourier space. Evaluation of the non-linear terms introduces aliasing errors and here the errors are eliminated using a simple truncation method (Canuto et al., 1988). At the code level, the Navier–Stokes equation is solved in the rotational form, which conserves kinetic energy and has been shown to be the most stable form for numerical simulations (Canuto et al., 1988). The temporal field is evaluated using a third-order Runge–Kutta scheme (Williamson, 1980). The time step is calculated according to a predefined Courant Freidricks Levy (CFL) number. All simulations in this study use the *CFL* number *CFL* = 0.75 and the time step Δt is adjusted dynamically during the simulation.

In order to obtain a statistically stationary simulation without decay of the energy spectrum, it is necessary to input energy by forcing the large scale motions of the flow. Several historical methods are available (Siggia and Patterson, 1978; Siggia, 1981; Kerr, 1985) but here the forcing scheme used is an Uhlenbeck–Ornstein stochastic process (Gardiner, 1985), as implemented by Eswaran and Pope (1987, 1988). Forcing of the large scales is achieved by the addition of a forcing acceleration to the Navier–Stokes equation in wave space form within a sphere of radius $K_F = 2\sqrt{2}\kappa_0$.

The Kolmogorov time scale, Taylor length scale and Taylor Reynolds numbers are calculated as – $\tau_\eta = (\nu_f/\varepsilon_f)^{1/2}$, $\lambda_f = (15\nu_f u_f'^2/\varepsilon_f)^{1/2}$, $\mathrm{Re} = u_f'\lambda_f/\nu_f$, respectively. The turbulent flow statistics for forced isotropic turbulence generated from this code were compared and validated with the results of Overholt and Pope (1996). Further validation work was performed by examining the energy density spectrum for the forced isotropic turbulence validation cases. Consistency with freely decaying turbulence is ensured by comparing with the experimental results of Comte-Bellot and Corrsin (1971). In all cases, the expected results were obtained and full details are available elsewhere (Scott, 2006).

2.1. Discrete phase method

The particle trajectories are calculated using the physical space velocity field, and advanced in time using the same third order Runge–Kutta scheme as used for the fluid phase. The position of a particle is calculated according to the following ordinary differential equation:

$$\frac{dX_i}{dt} = U_i \tag{2.1}$$

and the particle velocity is calculated using

$$\frac{dU_i}{dt} = -\frac{1}{\tau_U f_U}(U_i - u_i^*) \tag{2.2}$$

where u_i^* is the fluid velocity seen by the particle. The particles are assumed to be smaller than the Kolmogorov length scale of fluid flow (Maxey and Riley, 1983). The particle drag function f_U and particle Reynolds number Re_p are calculated as follows Clift and Grace (1978):

$$f_U = 1 + 0.15Re_p^{0.687} : Re_p = \frac{|U_i - u_i^*|\phi}{\nu_f} \leqslant 800 \tag{2.3}$$

where φ is the particle diameter. The particle relaxation timescale is defined,

$$\tau_U = \frac{18\rho_f \nu_f}{\rho_p \phi^2} \tag{2.4}$$

To calculate the particle drag force, it is necessary to know the instantaneous fluid velocity at the particle position. In the code, the instantaneous fluid velocity is interpolated to the particle position using a third order accurate polynomial (Ferziger and Peric, 1996).

2.2. Initialization and statistical analysis

All statistics were obtained from identical realizations of the turbulent carrier flow. Particles were initialized at random positions within the computational domain and released with initial velocity equal to the local fluid velocity. It was ensured that the particles were initialized in the same positions for each realization (assuming equal number of particles) and also ensured that the fluid realization was identical each time, independent of the number of particles used, since the flow is one-way coupled.

Both Eulerian and Lagrangian statistics were collected at every time step during the simulation. Lagrangian statistics were ensemble averaged across all particles. The Eulerian statistics were volume averaged for all nodes in the computational domain. An initial period at the start of the simulation was disregarded when time averaging to allow the particles to obtain a statistically stationary state within the flow.

A simple investigation was conducted to assess the influence of the particle population size on the accuracy of the measured statistics. The percentage errors for various measured statistics for 10^3, 10^4 and 10^5 particles relative to a reference simulation with 10^6 particles were calculated. In general this rough error assessment indicated that 10^4 particles should be sufficient for accurate Lagrangian mean statistics. This is supported by Elghobashi and Truesdell (1993) who found that 22^3 particles are sufficient. In practice, the additional CPU time required to simulate 10^5 particles is relatively small, so all simulations documented here were performed using 10^5 particles.

3. Results

Simulations were performed at Taylor Reynolds numbers of *Re* = 24.24, 49.28, 83.40, 136.0 using 32^3, 64^3, 128^3, 256^3 nodes, respectively, the flow characteristics of which are detailed in Table 1. For each Reynolds number, a range of Stokes numbers, based on the Kolmogorov timescale of the fluid, from 0.2–20 were considered. Although modification of the fluid phase turbulence is not accounted for in these simulations, the particle diameters have been selected to ensure particles are smaller than the Kolmogorov length scale of the flow.

Figs. 1 and 2 illustrate the tendency of inertial particles of a given *St* to accumulate in areas of low vorticity. In the *St* = 1.0 simulations the initially uniform particle field has organized itself into distinct areas of higher number density. Conversely the *St* = 10.0 simulations *appear* to maintain the initially uniform distribution.

All the measures used in this study confirm that preferential accumulation is maximum around Stokes number, $St \sim 1.0$. Fig. 3 shows the variation of PC with Stokes number for both the scale-dependent measure, D_c and scale-free measure, D_2. The D_c measure is inherently a scale-dependent measure and the bin-size used in

Table 1
Normalized Reynolds stresses and other quantities during the stationary period for forced isotropic turbulence. $\langle\cdot\rangle$ denote the time averaged stationary value.

		32^3	64^3	128^3	256^3
Largest resolved wave-number	$\kappa_{max}\langle\eta\rangle$	1.213	1.123	1.171	1.256
Smallest resolved wave-number	$\kappa_0\langle\eta\rangle$	0.0758	0.0351	0.0183	0.0085
Integral length scale	$\kappa_0\langle l\rangle$	1.224	1.005	0.8563	0.8109
Kolmogorov length scale	$\langle\eta/l\rangle$	0.0621	0.0350	0.0214	0.0105
Taylor micro-scale	$\langle\lambda/l\rangle$	0.5999	0.4846	0.3779	0.2417
Eddy turnover time	$T_E = \langle\lambda/u'\rangle$	1.486	0.3940	0.1375	0.0468
Kolmogorov time scale	$\langle\tau_\eta\rangle$	0.2301	0.0493	0.0134	0.0029
Start of stationary period	$T_S = T/T_E$	18.58	11.13	6.241	2.512
Duration of stationary period	$T_D = T_{max}/T_E - T_S$	164.8	94.85	23.09	3.019
Turbulent kinetic energy	$\langle k\rangle$	1.031	9.863	58.63	453.3
Dissipation rate	$\langle\varepsilon\rangle$	0.4821	10.45	141.7	2968.3
Taylor Reynolds number	$\langle Re_\lambda\rangle$	24.23	49.83	80.57	136.0

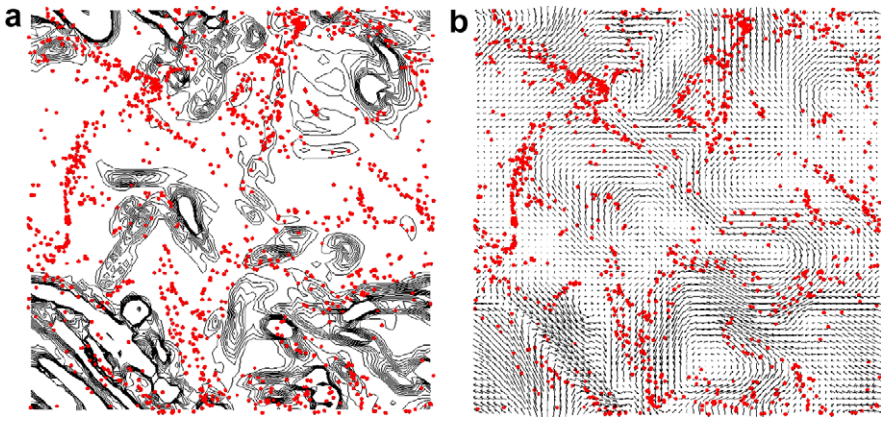

Fig. 1. (a) Contours of enstrophy and particle positions for a plane (contour levels between 0.2 $\langle e\rangle$ and 2.0 $\langle e\rangle$). (b) Fluid velocity vectors and particle positions for plane. ($Re = 50, St = 1.0$.)

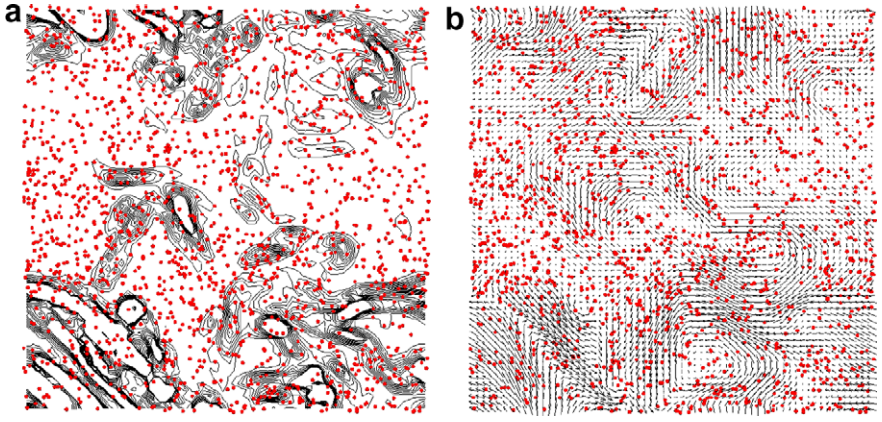

Fig. 2. (a) Contours of enstrophy and particle positions for a plane (contour levels between 0.2 $\langle e\rangle$ and 2.0 $\langle e\rangle$). (b) Fluid velocity vectors and particle positions for plane. ($Re = 50, St = 10.0$.)

Fig. 3 is nearly equal to the Kolmogorov length scale. On the other hand, the D_2 measure is simply the exponent of the scaling of number of particles N within a radius, r, from a base particle of the form $N\tilde{r}^{D_2}$. It is interesting to note that in spite of this inherent difference in the definition of D_c and D_2 measures, both peak at $St \sim 1$, as found by numerous previous studies. This demonstrates that preferential accumulation peaks at $St \sim 1$ irrespective of the measure used for quantifying it in our simulations and agrees with well-established conclusions to this effect from the literature.

Figs. 4 and 5 show the bin-size dependence of D and D_c measures for $Re = 50$. The bin-size has been normalized by the Kolmogorov length scale to enable estimation of the range of scales present in the calculation. It is observed that for the larger Stokes numbers, the peak of the D and D_c measures shifts to larger scales relative to the dissipation length scale. It has also been observed that the peak values of these measures for a given Stokes number decreases with increasing Reynolds number.

In order to facilitate comparison of our results, we used the same spatial scale for binning particles as that used by Wang and Maxey for estimating D_c in their simulations. Fig. 6 compares the D_c measure in our simulations with that of Wang and Maxey, where we use the same bin-size used by them for their $Re = 31$ calculation. It is seen that our results agree very well with those reported by Wang and Maxey. The Kolmogorov scaling of

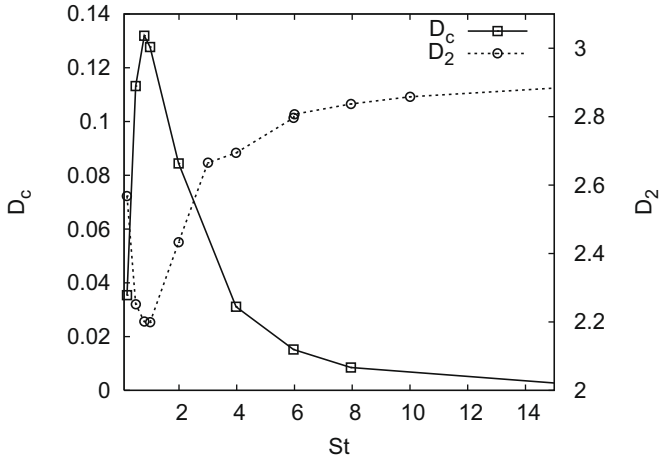

Fig. 3. Variation of D_c and D_2 measures with Stokes number. ($Re = 24$.)

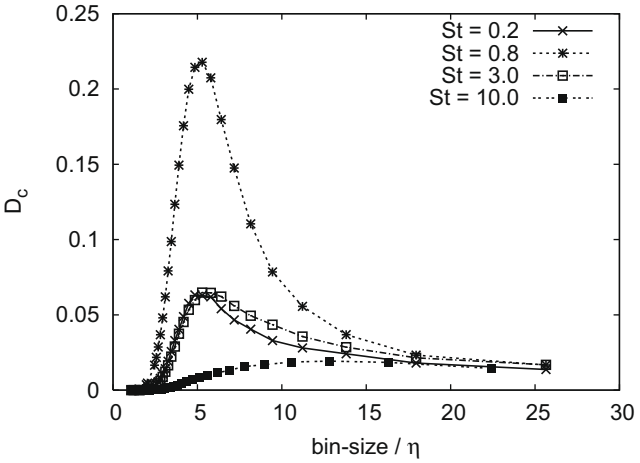

Fig. 4. Variation of D_c with normalized bin-size for $St = 0.2, 0.8, 3.0, 10.0$ for $Re = 50$.

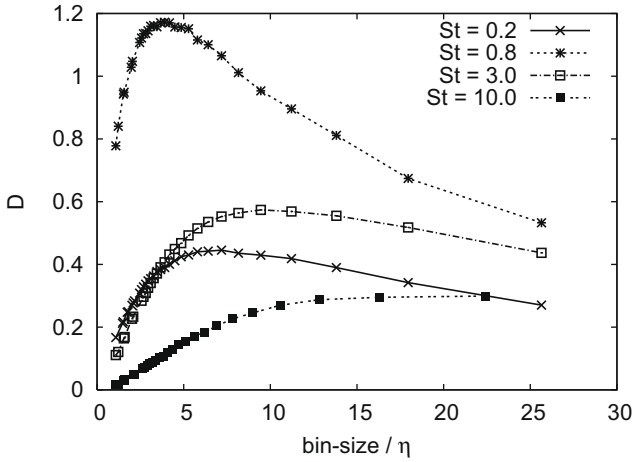

Fig. 5. Variation of D with normalized bin-size for $St = 0.2, 0.8, 3.0, 10.0$ for $Re = 50$.

preferential concentration phenomenon is also clearly evident with D_c showing a peak at Stokes number near unity for all the Reynolds numbers. It should be noted that in Fig. 6, the bin-size normalized by the Kolmogorov length scale, is different for each of the Reynolds numbers. Hence it would be erroneous to estimate the trend with *Re* based solely on Fig. 6. In order to estimate the

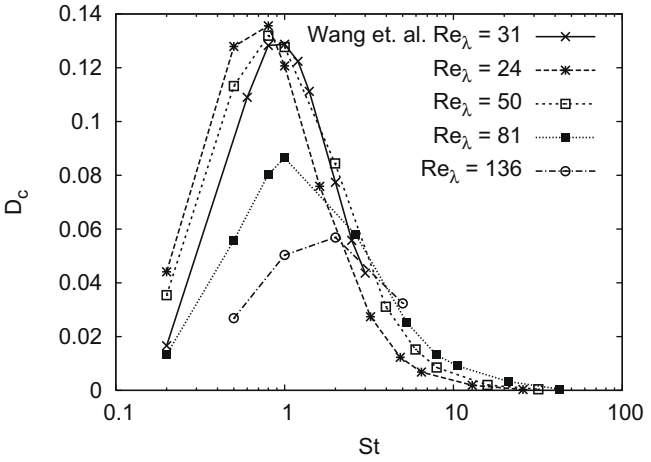

Fig. 6. Variation of D_c measure with Stokes number for $Re = 24, 50, 81, 136$ and compared with data from Wang and Maxey (1993).

trend with Reynolds number more clearly, it is required to investigate the trend of the peak values of D and D_c for a given *Re* and *St*. Fessler et al. (1994) reported the peak D values for their channel experiments and Fig. 7 compares results from our simulations with their experimental values. We observe a decrease in D measure for higher Reynolds number, for Stokes numbers, *St* less than 3. Moreover results from our simulations tend to the experimental results of Fessler et al. (1994) with increasing Reynolds numbers. Hogan and Cuzzi (2001) reported only a weak dependence on *Re* for the D_c measure in their simulations. However, it should be noted that in comparing D_c across Reynolds numbers, they had normalized their results with $St = 1$ measure and thus the qualitative variation of D_c with Stokes number showed invariance across Reynolds number, although this is not the case for this measure of PC.

In order to compare our PC estimation with the bulk of studies related to collision statistics of heavy particles, we calculated the correlation dimension (D_2) for each of our calculations and compared our results with that of Hogan and Cuzzi (2001) and Van Aartrijk and Clercx (2008). The D_2 measure derives itself from the radial distribution function (RDF), which itself is a statistical measure of clustering calculated from the particle position field. Fig. 8 shows the variation of D_2 with *St* for the different Reynolds numbers. The D_2 exhibits only a weak dependence of *Re*, consistent with similar conclusion by Collins and Keswani (2004). The D_2

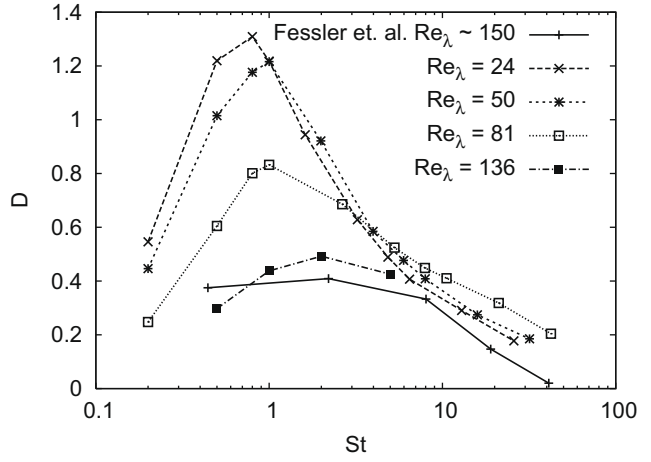

Fig. 7. Variation of D measure with Stokes number for $Re = 24, 50, 81, 136$ and compared with data from Fessler et al. (1994).

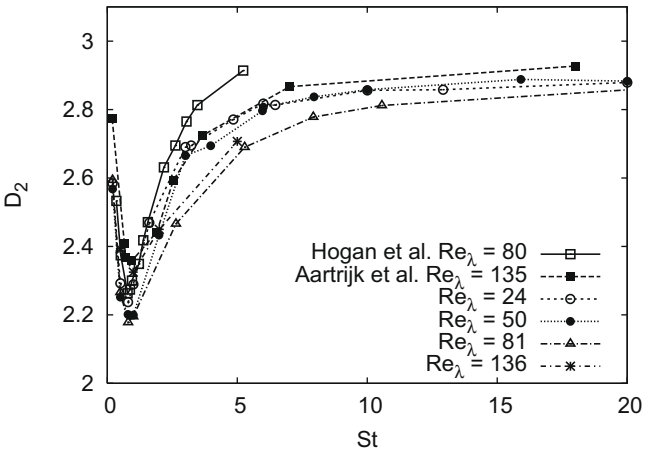

Fig. 8. Variation of D_2 measure with Stokes number for $Re = 24, 50, 81, 136$ and compared with data from Hogan and Cuzzi (1991) and van Aartrijk and Clercx (2008).

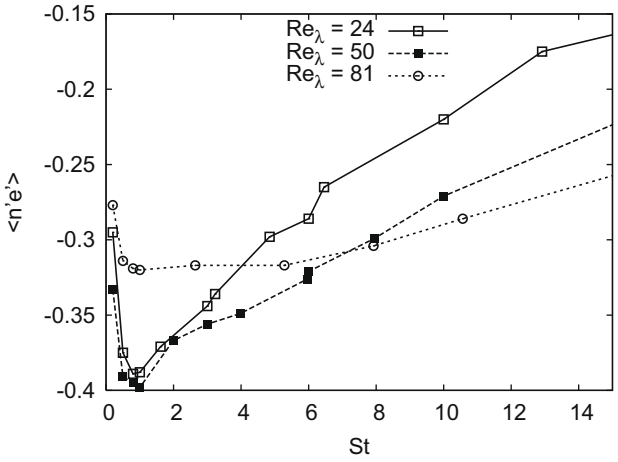

Fig. 9. Correlation coefficients of particle number density and fluid enstrophy in terms of *St* and *Re*.

measure is an indicator of particle–particle separation and captures the spacing between particles in a cluster. The observation that D_2 is only weakly dependent on *Re* means that the relative particle–particle separation is nearly independent of *Re*. With increasing *Re*, there is going to be a broader range of scales (eddy sizes) interacting with each other and the particles. In the simulations, it is evident that the dissipative scales (η) decrease by an order-of-magnitude from the smallest to highest *Re*. It is seen that the D_2 measure is insensitive to this range of eddy sizes since a single particle continues to see a similar structure around it. In short, the D_2 measure by virtue of its definition, strips out the quantitative scaling of particle separations, while retaining its qualitative structure, as it scales with *Re*.

In order to better probe the relation between the location of a particle and underlying fluid turbulence, we calculate the Eulerian correlation between local fluid enstrophy $e_f = \omega_k \cdot \omega_k$ and local particle number density *n*. The earliest studies of PC (Squires and Eaton, Fessler et al.) have shown that particles tend to reside in low-vorticity areas of the flow when they are preferentially concentrated. The correlation between number density and fluid enstrophy captures this phenomenon by an increasingly negative correlation between the two quantities. However, we are interested in the value of this indicator at higher Reynolds number, which is not so obvious. This scaling of this quantity ($\langle n'e' \rangle$) with Reynolds number is shown in Fig. 9. The general trend indicated is an increasing tendency for particles to accumulate in areas of low vorticity for particular particle Stokes numbers, as first observed by Squires and Eaton (1990a,b, 1991). In addition, the variation of the correlation between enstrophy and number density across the range of Stokes numbers considered is also less in the more turbulent simulations. It is evident that for the highest Reynolds number in the simulation, particles (of a greater range of response times) do not show a particular preference for low-vorticity areas. This is another pointer towards our argument of particle clusters becoming diffuse structures at the higher *Re* and *St*.

Squires and Eaton (1990a,b, 1991) suggest that as the particle Stokes number decreases, eventually a tracer limit will be reached and the accumulation effect is no longer evident. However, the studies of Squires and Eaton concentrated on a single turbulent Reynolds number whereas the present study has considered a range. Results from this study suggest that in addition to the tracer limit, the Reynolds number also has a significant effect on the preferential accumulation effect. In other words, as the turbulence level is increased for constant Stokes number, the accumulation effect appears to approach a limit as measured by D_2, but shows a scaling as measured by D and D_c quantities.

While the measures D_2 and $\langle n'e' \rangle$ are indicators of particle spacing and particle location vis-à-vis fluid enstrophy, respectively, they do not contain information about particle clusters and cluster separations. The bin-size dependence of D_c and D measures (Figs. 4 and 5) does provide information about particle clusters, though only in an approximate sense. It is seen that for a given Reynolds number, the range of sizes of particle clusters increases with Stokes number. At $St \sim 1$, we observe a sharp peak for these measures indicating that the particle number density field is composed predominantly of clusters of a single length scale. On the other hand, at higher Stokes numbers, there is an even distribution of clusters of all sizes. This is consistent with the observation by Yoshimoto and Goto (2007) and indicates that higher *St* particles interact with a range of eddy sizes. In this study, the same has been argued quantitatively for higher Reynolds numbers using additional measures.

In order to further investigate the idea of scaling of preferential accumulation with Reynolds number, the particle number density spectra were calculated during each simulation by taking the Fourier transform of the particle number density field. The clustering length scale, l_n, (Eq. (1.4)) is defined in consistence with the carrier flow integral scale l_f.

The variation of the clustering length scale across *St* for different *Re* is shown in Fig. 10. Note that in this figure, the highest Reynolds number data is not included owing to the computational expense of getting stationary statistics. From this figure it is clear that the clustering length scale shows the same trend as the other measures used in this study and shows a peak for $St \sim 1$. The clustering length scale basically refers to the distance between clusters of particles. At the peak of preferential accumulation, it is observed that the clustering length is highest. This suggests that PC is qualitatively composed of small particle clusters separated by relatively large distances. At the lowest Reynolds number in the simulation, there is a significant difference in the clustering length scale between the peak ($St \sim 1$) and that at higher Stokes numbers ($St \sim 20$). On the other hand, the difference in peak and the asymptotic value reached at higher St is much smaller for the highest Re. At higher Reynolds numbers, the particles interact with a broader range of fluid scales or eddy sizes. The smallest or Kolmogorov size eddies still play a dominant role leading to PC for appropriate particles ($St \sim 1$). However, for the more sluggish particles (higher *St*), the average spacing between particle clusters remains higher. It should be remembered that at the higher *Re* and *St*, the clusters

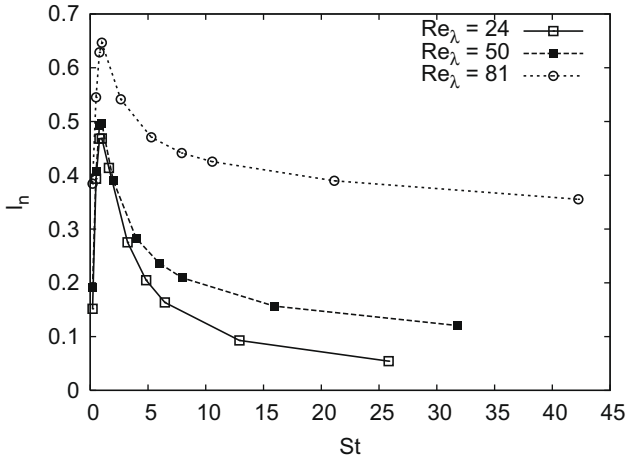

Fig. 10. Variation of clustering length scale with Stokes number for Re = 24, 50, 81.

themselves are larger or more diffuse structures, as seen from the shift in peak of D and D_c indicators towards larger length scales.

It is suggested that whilst the process of preferential accumulation is governed by the small scale features of the turbulence for the lower Reynolds numbers, while at higher Reynolds numbers, clustering is influenced by a range of eddy sizes, whish is most effectively demonstrated by the clustering length scale.

4. Conclusions

A pseudo-spectral DNS code with point-particles has been developed and has been validated for grid sizes up to 256^3 and shows good agreement with available experimental and computational data for simulation of isotropic turbulence. This code has been used to demonstrate the preferential accumulation effect of particles in areas of low vorticity using a new measure of preferential accumulation, the clustering length scale of accumulation.

The qualitative observations of preferential concentration as found by Squires and Eaton (1990a,b, 1991) are confirmed. The quantitative results are in agreement with the computational work of Wang and Maxey (1993) and experimental work of Fessler et al. (1994) using measures D_c and D used in their works respectively. The effect of bin-size on these measures has been systematically studied. It was observed that these measures show a decreasing trend with Re, irrespective of bin-size. The fact that this seems to suggest scaling with Reynolds number was further confirmed by measuring the correlation dimension, D_2. It has been noted, consistent with previous studies that D_2 shows only a weak dependence on Reynolds number. This seems to suggest that the D_2 measure provides a scale invariant picture of particle distribution. However it does not seem to capture the effect of the changes in the structure of particle number density field.

The structure of the particle number density distribution is effectively captured the clustering length scale defined in this work. The authors suggest that this measure better mimics the underlying fluid acceleration field. Recent works by Vassilicos and co-workers suggest the sweep-stick mechanism for preferential concentration, which presents a so-called fluid interpretation of accumulation. In the present work, the authors suggest a particle-interpretation for the same phenomenon.

References

Aliseda, A., Cartellier, A., Hainaux, F., Lasheras, J.C., 2002. Effect of preferential concentration on the settling velocity of heavy particles in homogeneous isotropic turbulence. J. Fluid Mech. 468, 77–105.

Balkovsky, E., Falkovich, G., Fouxon, A., 2001. Intermittent distribution of inertial particles in turbulent flows. Phys. Rev. Lett. 86 (13), 2790–2793.

Bec, J., Biferale, L., Cencini, M., Lanotte, A., Musacchio, S., Toschi, F., 2007. Heavy particle concentration in turbulence at dissipative and inertial scales. Phys. Rev. Lett. 98, 084502.

Boffetta, G., De Lillo, F., Gamba, A., 2004. Large scale inhomogeneity of inertial particles in turbulent flows. Phys. Fluids 16 (4), L20.

Boivin, M., Simonin, O., Squires, K.D., 1998. Direct numerical simulation of turbulence modulation by particles in isotropic turbulence. J. Fluid. Mech. 375, 235–263.

Canuto, C., Hussaini, M.Y., Quarteroni, A., Zang, T.A., 1988. In: Spectral methods in fluid dynamics. Springer series in computational physics. Springer, Berlin.

Chen, L., Goto, S., Vassilicos, J.C., 2006. Turbulent clustering of stagnation points and inertial particles. J. Fluid Mech. 553, 143–154.

Clift, R., Grace, J.R., 1978. Bubbles, Drops and Particles. Academic Press, New York.

Collins, L.R., Keswani, A., 2004. Reynolds number scaling of particle clustering in turbulent aerosols. New J. Phys. 6, 119.

Comte-Bellot, G., Corrsin, S., 1971. Simple time correlations of full and narrow-band velocity signals in grid generated isotropic turbulence. J. Fluid Mech. 48, 273–337.

Eaton, J.K., Fessler, J.R., 1994. Preferential concentration of particles by turbulence. Int. J. Multiphase Flow 20, 169–209.

Elghobashi, S., Truesdell, G.C., 1992. Direct simulation of particle dispersion in a decaying isotropic turbulence. J. Fluid Mech. 242, 655–700.

Elghobashi, S., Truesdell, G.C., 1993. On the two-way interaction between homogeneous turbulence and dispersed solid particles I: Turbulence modification. Phys. Fluids 5, 1790–1801.

Eswaran, V., Pope, S.B., 1987. An examination of forcing in direct numerical simulations of turbulence. Comput. Fluids 16 (3), 257–278.

Eswaran, V., Pope, S.B., 1988. Direct numerical simulation of the turbulent mixing of a passive scalar. Phys. Fluids 31 (3), 506–520.

Ferziger, J., Peric, M., 1996. Computational Methods for Fluid Dynamics. Springer-Verlag.

Fessler, J.R., Kullick, J.D., Eaton, J.K., 1994. Preferential concentration of heavy particles in a turbulent channel flow. Phys. Fluids 6 (11), 3742–3749.

Gardiner, C.W., 1985. Handbook of stochastic methods for physics, chemistry and the natural sciences. Springer series in synergetics. Springer.

Goto, S., Vassilicos, J.C., 2008. Sweep-stick mechanism of heavy particle clustering in fluid turbulence. Phys. Rev. Lett. 100, 054503.

Grassberger, P., Procaccia, I., 1983. Measuring the strangeness of strange attractors. Physica D 9, 189–208.

Hogan, R.C., Cuzzi, J.N., 2001. Stokes and Reynolds number dependence of preferential particle concentration in simulated three-dimensional turbulence. Phys. Fluids 13 (10), 2938–2945.

Kerr, R.M., 1985. Higher-order derivative correlations and the alignment of small-scale structures in isotropic numerical turbulence. J. Fluid Mech. 153, 31.

Maxey, M.R., Riley, J.J., 1983. Equation of motion for a small rigid sphere in a uniform flow. Phys. Fluids 26, 883–889.

Orszag, S.A., Patterson, G.S., 1972. Numerical simulation of three-dimensional homogeneous isotropic turbulence. Phys. Rev. Lett..

Overholt, M.R., Pope, S.B., 1996. Direct numerical simulation of a passive scalar with imposed mean gradient in isotropic turbulence. Phys. Fluids 8 (11), 3128–3148.

Rogallo, R.S. 1981. Numerical experiments in homogeneous turbulence. Technical Report 81315, NASA.

Scott, S.J., 2006. PDF based method for modelling polysized particle laden turbulent flows without size class discretisation, Ph.D. Thesis, Imperial College London.

Shaw, R.A., 2003. Particle-turbulence interactions in atmospheric clouds. Annu. Rev. Fluid Mech. 35, 183–227.

Siggia, E.D., 1981. Numerical study of small-scale intermittency in three-dimensional turbulence. J. Fluid Mech., 107–375.

Siggia, E.D., Patterson, G.S., 1978. Intermittency effects in a numerical simulation of stationary three-dimensional turbulence. J. Fluid Mech 86, 567.

Squires, K.D., Eaton, J.K., 1990a. Preferential concentration of particles by turbulence. Phys. Fluids 3, 1169–1178.

Squires, K.D., Eaton, J.K., 1990b. Particle response and turbulence modification in isotropic turbulence. Phys. Fluids A 2, 1191–1203.

Squires, K.D., Eaton, J.K., 1991. Measurements of particle dispersion obtained from direct numerical simulations of isotropic turbulence. J. Fluid Mech., 1–35.

Sundaram, S., Collins, L.R., 1997. Collision statistics in an isotropic particle-laden turbulent suspension. Part 1. Direct numerical simulations. J. Fluid Mech. 335, 75–109.

Tang, L., Wen, F., Yang, Y., Crowe, C.T., Chung, J.N., Troutt, T.R., 1992. Self-organizing particle dispersion mechanism in a plane wake. Phys. Fluids A 4 (10), 2244–2251.

Van Aartrijk, M., Clercx, H.J.H., 2008. Preferential concentration of heavy particles in stably stratified turbulence. Phys. Rev. Lett. 100, 254501.

Wang, L.P., Maxey, M.R., 1993. Settling velocity and concentration distribution of heavy particles in isotropic turbulence. J. Fluid Mech. 256, 27–68.

Wang, L.P., Wexler, A.S., Zhou, Y., 2000. Statistical mechanical description and modelling of turbulent collision of inertial particles. J. Fluid Mech. 415, 117–153.

Williamson, 1980. Low storage Runge–Kutta schemes. J. Comput. Phys. 35, 48–56.

Wood, A.M., Hwang, W., Eaton, J.K., 2005. Preferential concentration of particles in homogeneous and isotropic turbulence. Int. J. Multiph. Flow 31, 1220–1230.

Yoshimoto, H., Goto, S., 2007. Self-similar clustering of inertial particles in homogeneous turbulence. J. Fluid Mech. 577, 275–286.